ELSEVIER

Journal of Molecular Catalysis A: Chemical 169 (2001) 147–155

JOURNAL OF MOLECULAR CATALYSIS A: CHEMICAL

www.elsevier.com/locate/molcata

Photocatalytic degradation of *o*-cresol sensitized by iron–titania binary photocatalysts

Bonamali Pal*, Tomohiro Hata, Kouichi Goto, Gyoichi Nogami

Department of Electrical Engineering, Kyushu Institute of Technology, Tobata-ku, Kitakyushu-804, Japan

Received 23 August 2000; received in revised form 21 November 2000; accepted 21 November 2000

Abstract

The degradation of *ortho*-cresol (*o*-cresol) assisted by Fe/TiO_2 photocatalysts was investigated in oxygenated aqueous suspension in a spiral glass flow reactor. Iron–titania (1–10 wt.% Fe) mixed catalysts have been prepared by sol–gel impregnation method using metal alkoxide precursors. The surface structure of Fe/TiO_2 catalyst was studied by surface analysis with XPS and TEM techniques. Characterization of these catalysts, fired at different temperatures (in the range 500–900°C) using X-ray diffraction (XRD) showed that the sintering temperature and incorporation of iron ions mediate the phase transformation and growth of pseudobrookite (Fe_2TiO_5) phase at higher temperatures. The rate of degradation of *o*-cresol decreases with the increasing sintering temperature and iron content of the catalysts and the initial pH of the aqueous solution of *o*-cresol changes with the illumination time due to the formation of various acidic intermediate photoproducts.

Keywords: Iron–titania catalysts; Cresol degradation; Photocatalysis; Binary mixed oxides

1. Introduction

The use of semiconductor particles as photocatalysts for the degradation of toxic organic chemicals continues to be an active area of investigation [1–4]. A number of studies [5–8] have been carried out on iron–titania powders for their photoactivity in catalytic processes. Mixed phase Ti/Fe metal oxide colloids containing 0.1–50 at.% Fe have been investigated [9] for the enhancement of catalytic properties and spectral range. The photocatalytic activity of iron doped TiO_2 or mixed oxides of Fe and Ti, prepared by impregnation and coprecipitation methods has been shown to be more active for $CHCl_3$ oxidation [10], EDTA oxidation [11], degradation of oligocarboxylic acid [12], and 4-nitrophenol degradation [13], etc. The photooxidation of neat toluene to benzaldehyde, benzyl alcohol and benzoic acid was achieved [14] using 0.5 and 5 wt.% iron doped TiO_2 prepared by impregnation method [15]. More recently, Zhang et al. deduced [16] the photoinduced interfacial charge transfer mechanism of TiO_2/Fe_2O_3 composite film which showed modified photovoltaic response due to the cooperative effect of the heterojunction at TiO_2/Fe_2O_3 interface.

Most attempts were aimed at synthesizing iron–titania photocatalysts by impregnation method involving the hydrolysis of Ti-alkoxide in the presence of different Fe(III) compounds in aqueous solution. The fact that the use of Fe dopant materials and the hydrolysis technique prior to mixing of metal precursors,

* Corresponding author. Present address: Catalysis Research Center, Hokkaido University, Sapporo 060-0811, Japan.
Fax: +81-11-706-4925.
E-mail address: pal@cat.hokudai.ac.jp (B. Pal).

1381-1169/01/$ – see front matter
PII: S1381-1169(00)00549-5

strongly influences the photocatalytic activity due to the nature of iron distribution on the resulting particles formed. In this context, the present study was targeted to prepare Fe/TiO_2 catalysts with the thorough distribution of iron incorporation into the growing particles by mixing the metal alkoxide precursors prior to their hydrolysis. This effect may led to improve the charge separation at the interface of the resulting particles due to the formation of efficient charge trapping sites. A correlation between physicochemical properties and photocatalytic activity was conducted using the photodegradation reaction of *ortho*-cresol (*o*-cresol) as a model compound which was studied [17–19] in aqueous TiO_2 and polyoxotungstate suspensions using slurry reactor with bulk illumination. The illumination factor is also one of the most important parameter which influences the catalytic activity. The high illuminated specific catalyst surface area and uniform distribution of light for catalyst illumination are highly desirable for efficient photocatalytic reaction which was provided in the present study using black light blue fluorescent tube, inserted into the middle of a narrow bore Pyrex spiral glass tube with the continuous flow of reaction solution.

2. Experimental procedures

Ortho-cresol, titanium(IV) isopropoxide and Fe(III) acetylacetonate, isopropanol and all other chemicals were of AnalaR grade. The mixed oxide was prepared by sol–gel impregnation methods using titanium(IV) isopropoxide and Fe(III) acetylacetonate as organic precursors. The samples had nominal concentration of 1, 5 and 10 wt.% of iron with respect to the weight of titania. The catalyst was prepared as follows: Desired amount of Ti-tetraisopropoxide was added drop-wise to the solution of 20 ml isopropanol at 0°C with constant stirring. Similarly, calculated amount of Fe(III) acetylacetonate was dissolved in 20 ml isopropanol and then it was mixed with the isopropanolic solution of Ti-tetraisopropoxide dropwise with vigorous stirring. The mixture was kept for 24 h with constant stirring and then aqueous solution of HNO_3 was added slowly over the course of 30 min in to the well agitated system at room temperature. The solvent was allowed to slowly evaporate from the system by keeping the sol over hotplate with magnetic stirrer. The resulting powder mixtures thus obtained, were then grounded in mortar pestle and sintered at 500, 700 and 900°C for 10 h.

The mixed oxide was characterized by X-ray diffraction (XRD), X-ray photoelectron spectroscopy (XPS), transmission electron microscopic technique (TEM) and photocatalytic properties were tested towards the decomposition of *o*-cresol in aqueous suspension using a continuous flow spiral glass photoreactor.

X-ray diffraction patterns were recorded on a JEOL diffractometer with Ni-filtered Cu Kα radiation. The instrument employed for the XPS studies was JEOL spectrometer operating with pass energy of 50 eV. It consists of an ultrahigh vacuum chamber (UHV) with a built in high pressure cell which allows switching the sample from the high pressure cell to the UHV system without exposing it to air. O 1s, Ti 2p and Fe 2p XP spectra were recorded using Mg Kα radiation as the excitation source.

In a typical photocatalytic experiment, 150 ml (50 ppm) aqueous solution of *o*-cresol was mixed with 100 mg Fe/Ti mixed oxide (sintered at various temperatures) in a conical flask and the solution was stirred continuously (by magnetic stirrer) with the purging of excess oxygen. The resultant mixture from the conical flask was circulating through a Pyrex glass tube of 5.5 m length and 0.4 cm i.d. (which was wound 41 times to form a spiral coil) at constant flow rate with the help of a peristaltic pump. Silicon tube was fitted to the inlet and outlet ports to allow circulation of the solution through the conical flask. A 15 W black light blue fluorescent tube (FL-15 BL) was inserted into the middle of the spiral glass coil as an irradiation source. In the continuous recirculation mode experiments, aliquots (5 ml) were retrieved from the reservoir at certain time intervals and analyzed after filtering through (0.2 mM) Millipore filter. The solution was returned to the reservoir after each analysis. The concentration of the unreacted *o*-cresol was analyzed with UV–VIS spectrophotometer by measuring its absorbance at 270 nm.

3. Results and discussion

3.1. X-ray diffraction analysis

Fig. 1 shows the XRD patterns of 1 wt.% Fe doped titania powders sintered at 500, 700 and 900°C for 10 h

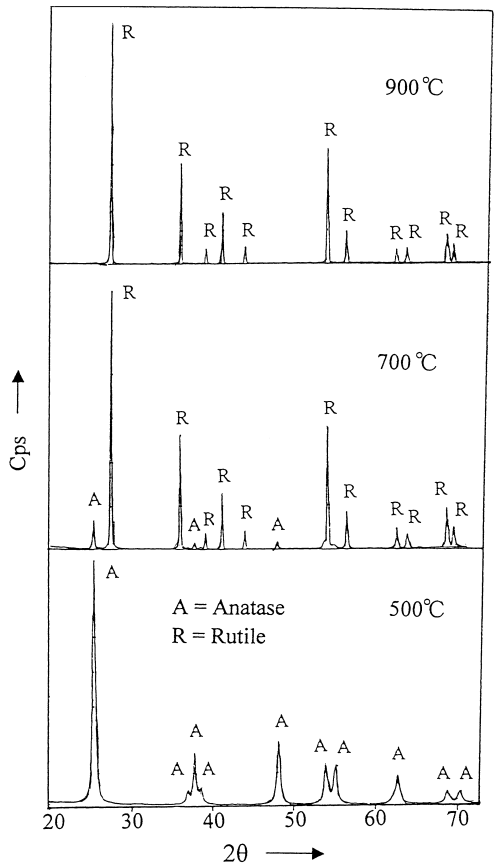

Fig. 1. XRD patterns of 1 wt.% Fe/TiO_2 oxides sintered at different temperatures.

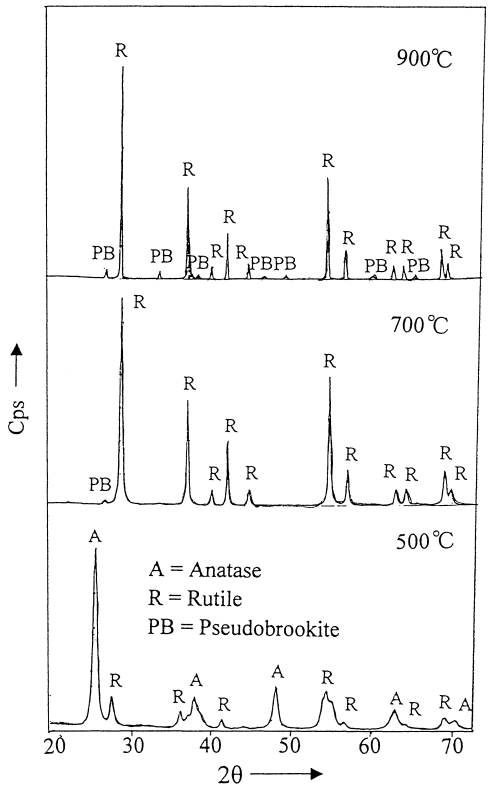

Fig. 2. XRD patterns of 5 wt.% Fe/TiO_2 oxides sintered at different temperatures.

in air atmosphere. It has been revealed from the XRD patterns that the main phases present are pure anatase at 500°C, mixture of anatase and rutile at 700°C and pure rutile phase at 900°C. No pseudobrookite phase was found at this low iron concentration (1 wt.%) and temperature range. The X-ray photographs of 5 wt.% Fe/Ti oxide samples (Fig. 2) show the presence of anatase and rutile at 500°C, rutile and increasing amount of pseudobrookite phases at 700 and 900°C, respectively. The same trend was also observed in the case of 10 wt.% Fe/Ti samples with higher percentage of pseudobrookite phase at high sintering temperatures (700 and 900°C) along with the rutile phases.

An increase in the firing temperature favors [20,21] the anatase to rutile transition, together with the reaction of iron and titanium oxides and the growth of the individual crystals. The anatase-rutile transformation seems to become marked only above 500°C in the case of 1 wt.% Fe/TiO_2 specimens and the increasing percentage of rutile phase was observed in heavily loaded iron samples at lower temperature (500°C) which evidencing the catalytic role of Fe ions in promoting the anatase-rutile transformation. It has been reported [22–24] that in TiO_2 supported systems the anatase to rutile transformation occurs at a lower temperature as compared to pure anatase because of the catalytic effect of transition metal ions. During phase transition, the elongated anatase crystal form rearranges to the shorter rutile form. This process involves a rearrangement of the majority of Ti^{4+} ions by rupture of two of the six Ti–O bonds in the unit cell to form new bonds [25,26]. The rupture of these bonds and the simultaneous phase transition results in highly disorder state where rapid migration of titanium-oxygen species,

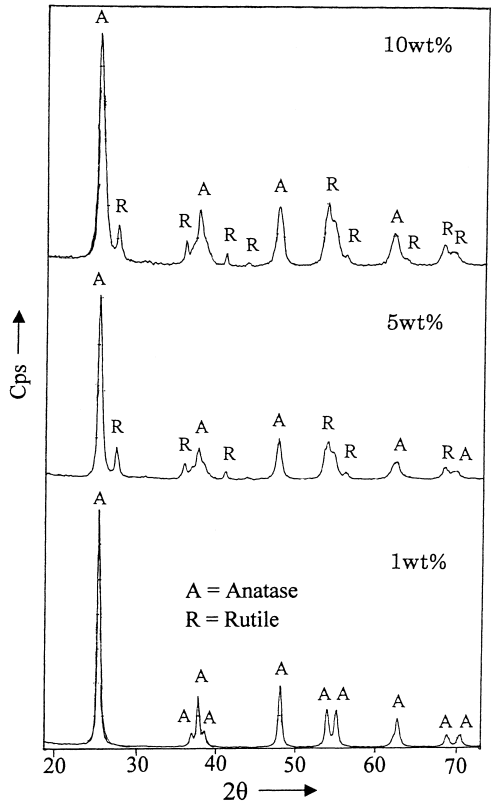

Fig. 3. XRD patterns of different Fe/TiO_2 oxides sintered at 500°C.

titanium ions and oxygen ions is occurring. These migrating species encounter with the incoming (inward diffusion to the TiO_2 lattice) iron oxide particles, and are stabilized by reaction with them to form a mixed surface oxide (Fe_2TiO_5).

It has been observed from the XRD patterns that the progressive development of crystallinity occurs with increasing sintering temperatures of the powder samples and the broadness of the peaks decreases with the increasing firing temperatures. Moreover, it should also be noted from the XRD patterns of Fig. 3 that with the increasing iron contents of the specimens fired at the same temperature (500°C), the broadness of the peaks increases which indicated that particle size had increased and it was suggested [27–29] that at high temperatures, the metal may diffuse into titania support which causes broadening of the X-ray lines. These results could indicate that effect of iron contents also reflects the behavior of the specimens about its crystalline nature and particles size distribution. The diffractograms of all the specimens fired 900°C show that with iron concentration more than 1 wt.%, detectable amount of Fe_2TiO_5 phase is formed which is characterized by its strong and sharp peaks. This results are in agreement with other works [22,30,31] where it has been observed that at low iron concentration, Fe^{3+} ions are well dispersed in the lattice substitutionally and at higher loading of Fe systems become multiphasic with the formation of Fe_2TiO_5 phase at higher temperatures.

However, the XRD data does not show any segregation of bare Fe_2O_3 peaks in our newly developed sol–gel Fe/TiO_2 catalyst specimens. This surface enrichment of iron oxide is also supported by very low intense peak of Fe 2p (binding energy shifted) in the XP spectra and TEM surface morphology measurements discussed in the following section. In our earlier studies [32] of Fe_2O_3/TiO_2 mixed oxide system, we also confirmed by FTIR a spectroscopic band at 538.6 cm^{-1} as compared to 542.6 cm^{-1} in bare Fe_2O_3, which was ascribed to surface enriched Fe_2O_3 species in the Fe/Ti mixed oxide specimens.

3.2. TEM and XPS studies

TEM photographs of the iron–titania samples calcined at different temperatures with various iron contents are shown in Fig. 4. It can be observed that large aggregates and clusters of particles distributed randomly at lower temperatures. The TEM photographs (Fig. 4a and b) of 1 wt.% Fe/TiO_2 sample fired at 500 and 900°C showed that at low temperature the particles are of amorphous nature and at high temperature, particles are somewhat crystalline with smaller aggregates. An increase in the sintering temperature, the gradual development of the crystallinity is observed. The same trend was also observed (Fig. 4c) in the case of 5 wt.% samples sintered at 900°C. This is in agreement with the XRD results where broad and sharp peaks appeared with increasing sintering temperature of the samples due to the increase of crystal size. The TEM photographs show that most of the particles are enriched with other types of specimens and some lattice fringes are observed due to the overlapping crystallites. This may be due to presence of coexisting Fe_2O_3/TiO_2 particles pair-wise association or due to the enrichment of one species

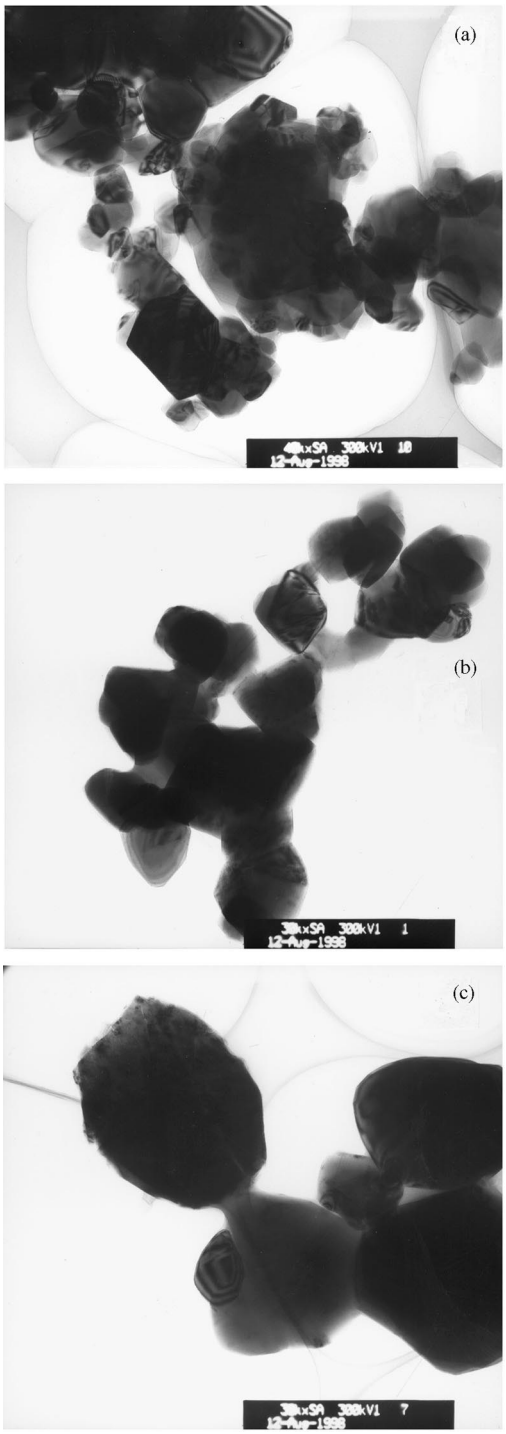

Fig. 4. TEM micrographs (1 cm = 330 nm) of 1 wt.% Fe/TiO_2 oxides, sintered at (a) 500°C; (b) 900°C and (c) 5 wt.% Fe/TiO_2 oxides sintered at 900°C temperature.

(Fe_2O_3) to the surface of others (Fe/TiO_2 specimens) which can be clearly seen separately in the TEM photograph of Fig. 4b and c. Furthermore, it can also be observed that some islands of materials are embedded on the large crystallite which was probably undergoing diffusion process in the titania lattice.

Fig. 5 (spectra I and II) shows the variation in intensity and shape of Fe 2p and Ti 2p XP spectra of 5 wt.% iron loaded titania samples sintered at different temperatures. It reveals that with the increasing sintering temperatures, the shape and intensity of both the spectra changes due to the interaction of this metal oxide specimens which results in the formation of new phases in the surface layer due to the diffusion of Fe into the titania lattice. The binding energy of Fe 2p (711–12.5 eV) values also somewhat shifted [28] compared to pure 2p (710.7 eV) spectra in Fe_2O_3 which indicated that Fe_2O_3 is impregnated into TiO_2 whose Ti 2p BE values lies in the range of 458–460 eV which reveals that majority of the Ti species are present in the 4+ oxidation states. Also it has been observed that the Fe $2p_{3/2}$ spectral intensity is somewhat less at higher temperature compare to low temperature treatment. This experimental observation suggests that Fe ion diffusion is a facile process [33,34] in the Ti lattice at higher temperature (>700°C). XP spectra of Fig. 5 (spectra III and IV) also shows the change of binding energy (in the range of 531–532 eV) of O 1s of Fe/Ti oxide samples as a function of iron content and sintering temperature. Decrease in spectral area and intensity of O 1s spectrum with the increasing sintering temperature and decreasing iron content can be attributed [22,35] to the restructuring of surface phase and crystallinity in the oxide species due to the formation of iron rich surface layers containing Fe_2TiO_5 and Fe_2O_3 in addition to the solid solution of Fe^{3+} in TiO_2.

4. Photocatalytic degradation of *o*-cresol

The Photocatalytic activity of mixed oxide samples fired at different temperature was tested for the degradation of aqueous solution of *o*-cresol. The effect of photocatalytic activity of Fe/TiO_2 oxide fired at different temperatures on the rate of destruction of *o*-cresol is shown in Fig. 6. It can be observed that

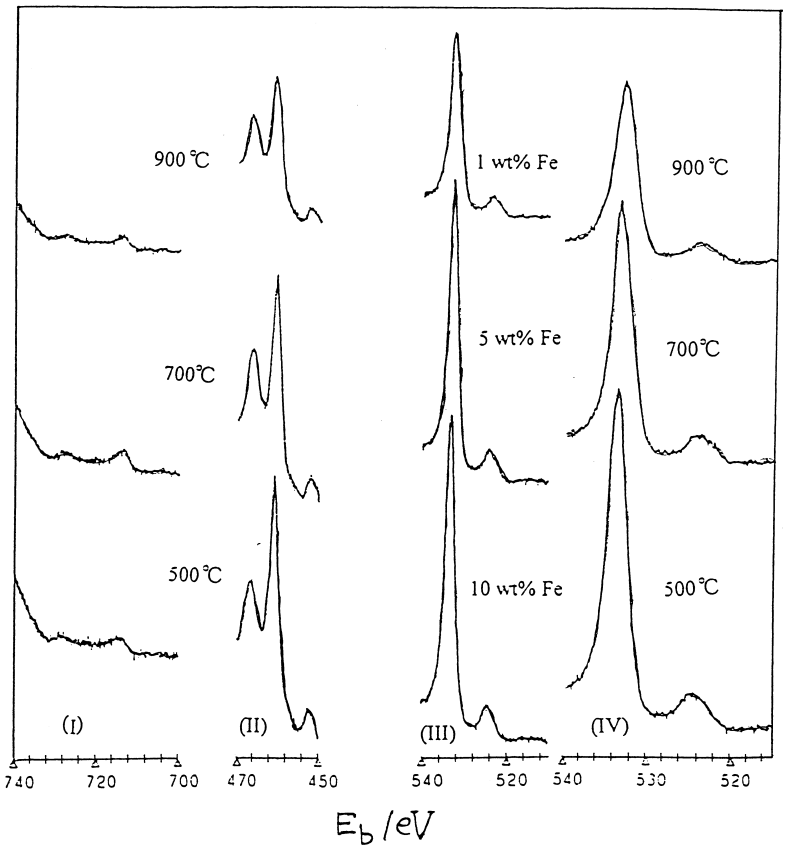

Fig. 5. XP spectra of (I) Fe 2p and (II) Ti 2p of 5 wt.% Fe/TiO_2 samples sintered at different temperatures and O 1s spectra of (III) different Fe/TiO_2 oxide samples sintered at 900°C, and (IV) 5 wt.% Fe/TiO_2 oxides as a function of sintering temperatures.

absorbance is gradually decreasing with the illumination time due to the degradation of cresol. The rate of degradation is mostly very rapid at lower temperature compared to sample treated at high temperature. All the Fe/TiO_2 specimens fired at 500°C, showed comparably same reactivity irrespective of iron loadings and the catalyst with higher loaded iron showed significantly different reactivity at higher temperatures. Fig. 6a reflects the photocatalytic behavior of 1 wt.% Fe loaded samples sintered at different temperatures. The degradation rate decreases with the sintering temperature due to the presence of different crystalline phases (anatase and rutile) at various temperature as observed in XRD analysis. Fig. 6b (5 wt.% Fe samples) reveals that catalytic activity is highly reduced at 900°C due to presence of higher amount of surface enriched iron oxide and inactive pseudobrookite phases in comparison to 1 wt.% sample fired at the same temperature. Similarly, the catalyst sintered at 700°C also shows reduced activity due to the presence of isolated rutile and trace amount of pseudobrookite phases compared to both anatase and rutile phases of 1 wt.% samples fired at the same temperature. It was noted that the photocatalytic activity of 10 wt.% Fe/TiO_2 sintered at 700 and 900°C is highly decreasing at the same extent. Due to the gradual development of rutile phase, surface enriched iron oxide phase and Fe_2TiO_5 phase with increasing particle size at higher firing temperatures, the catalytic activity reduces to a great extent. Also, due to low mobility, photoexcited electrons in the mixed phases may enhance [11,21] the recombination rate because the average distance

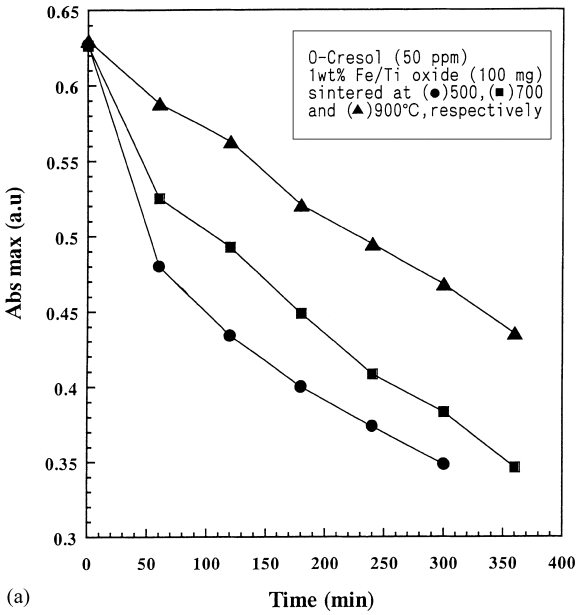

Fig. 6. Effect of photocatalytic activity of (a) 1 wt.% and (b) 5 wt.% Fe/TiO_2 oxide catalysts sintered at various temperatures.

between the trap sites decreases with increasing number of dopants within the particles. It was observed that pH changes (from 6.2 to 4.4) rapidly with the irradiation time in case of 500°C samples due to the formation of intermediate products owing to its higher reactivity compared to samples treated at higher temperatures where pH change (from 6.2 to 5.4) is not so significant.

Some of the intermediates were identified by a gas chromatograph/mass spectrometer (GC/MS) after extracting the aqueous solutions with diethyl ether. The mass spectra (Fig. 7) shows many fragmentation peaks. We were unable to characterize all *m/z* fragmentation value. The obtained *m/z* value 145 and 91 in the mass spectra correspond to $M + 1$ fragmentation of unsaturated adipic acid (molecular weight, $M = 144$) and $M + 1$ fragmentation of oxalic acid ($M = 90$), respectively. Possibly, these intermediate photoproducts are generated from the primary intermediates (*o*-hydroxy benzyl alcohol or hydroxy benzoic acid) which seem to results [14,18] from the direct attack of OH radicals to the CH_3 group of cresol because no acetic acid was detected in the reaction solution. Subsequent hydroxylation or direct oxidation by positive holes at the semiconductor surface may lead to the formation of those dicarboxylic acids which represent fragments resulting from the aromatic ring opening. It is not clear why the intermediate products distribution reported here is so markedly different from those cases of TiO_2 mediated [17,19] reactions of cresol where mainly hydroxylated products, e.g. methylcatechol and methylhydroquinone and hydroxy benzaldehyde were identified. One of the most important reasons is the nature of catalyst used in this present study whose surface acidity, crystallinity, and electronic environment (heterojunction of TiO_2/Fe_2O_3 system) may induce the different catalytic site compared to bare titania catalyst. Finally, the initial pH is around six in the present work compared to most study carried out [17,19] at alkaline or acidic pH which significantly change the adsorption site due to the variation of surface charge at the catalysts/substrate interface which may have detrimental effect on the degradation kinetics. The photocatalytic experiments indicated that dopant concentration has no detrimental effect on the catalytic activity of Fe/TiO_2 specimens fired at low temperature. However, structural effects and surface properties play a key role to the photoreactivity which became less and less significant as the iron content and temperature increased because surface composition deviated strongly from bulk composition irrespective of the preparation technique.

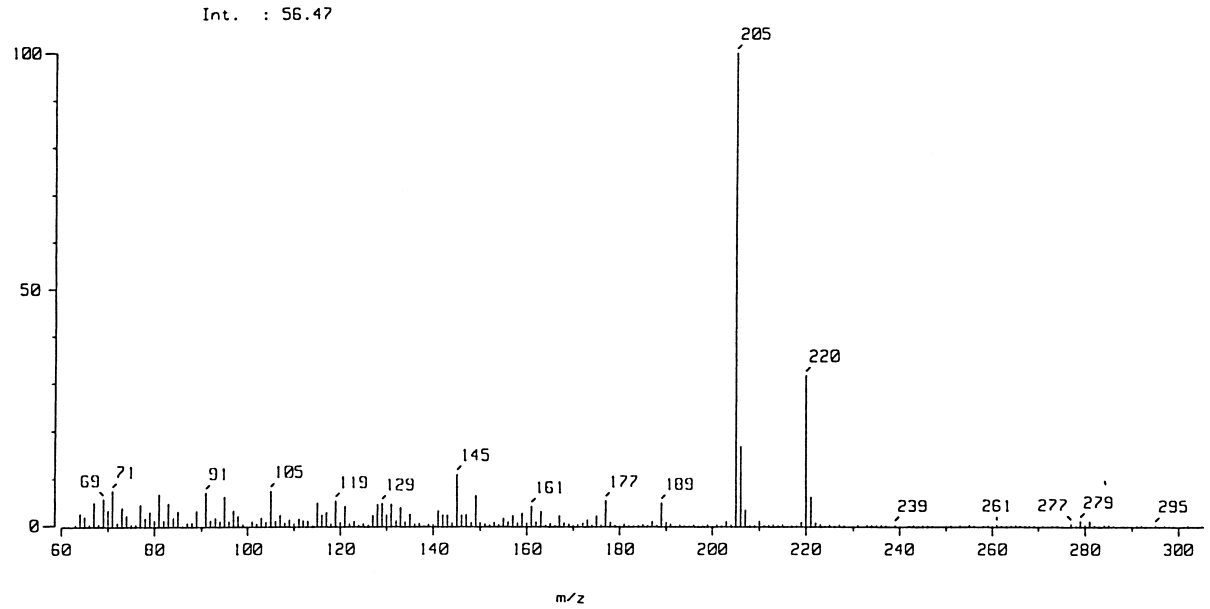

Fig. 7. GC/MS spectra of the plausible intermediate products formed, during degradation of *o*-cresol using 1 wt.% Fe/TiO_2 oxide samples fired at 500°C.

Acknowledgements

We are very much thankful to the staff of Instrumental Analysis Center of Kyushu Institute of Technology, Japan for their timely help in many experimental works. One of us (BP) is grateful to the Ministry of Education, Government of Japan, for offering a MONBUSHO fellowship.

References

[1] M.R. Hoffmann, S.T. Martin, W. Choi, D.W. Bahnemann, Chem. Rev. 95 (1995) 69.
[2] D.F. Ollis, N. Serpone, in: N. Serpone, E. Pelizzetti (Eds.), Photocatalysis: Fundamentals and Applications, Wiley, New York, 1989, p. 603.
[3] J.M. Herrmann, Catal. Today 53 (1999) 115.
[4] R.W. Mathews, J. Catal. 111 (1988) 264.
[5] N. Serpone, D. Lawless, Langmuir 10 (1994) 643.
[6] M.I. Litter, J.A. Navío, J. Photochem. Photobiol. A: Chem. 98 (1996) 171.
[7] J.A. Navío, J.J. Testa, P. Djedjeian, J.R. Padrón, D. Rodríguez, M.I. Litter, Appl. Catal. A: General 178 (1999) 191.
[8] D.W. Bahnemann, Isr. J. Chem. 33 (1993) 115.
[9] D.W. Bahnemann, D. Bockelmann, R. Goslich, M. Hilgendorff, D. Weichgrebe, in: D.F. Ollis, H. Al-Ekabi (Eds.), Photocatalytic Purification and Treatment of Water and Air, Elsevier, Amsterdam, 1993, p. 301.
[10] W. Choi, A. Termin, M.R. Hoffmann, J. Phys. Chem. 98 (1994) 13669.
[11] M.I. Litter, J.A. Navío, J. Photochem. Photobiol. A: Chem. 84 (1994) 183.
[12] J.A. Navío, G. Colón, M.I. Litter, G.N. Bianco, J. Mol. Catal. A. Chem. 106 (1996) 267.
[13] L. Palmisano, M. Schiavello, A. Sclafani, C. Martin, I. Martin, V. Rives, Catal. Lett. 24 (1994) 303.
[14] J.A. Navío, M. García Gómez, M.A. Pradera Adrián, J. Fuentes Mota, in: Guisnet et al. (Eds.), Heterogeneous Catalysis and Fine Chemicals Vol. II, Elsevier, Amsterdam, 1991, p. 445.
[15] J.A. Navío, M. Macías, M. González-Catalán, A. Justo, J. Mater. Sci. 27 (1992) 3036.
[16] X. Zhang, Y. Cao, S. Kan, Y. Chen, J. Tang, H. Jin, Y. Bai, L. Xiao, T. Li, B. Li, Thin Solid Films 327/329 (1998) 568.
[17] R. Terzian, N. Serpone, C. Minero, E. Pelizzetti, J. Catal. 128 (1991) 352.
[18] A. Mylonas, E. Papaconstantinou, Polyhedron 15 (1996) 3211.
[19] K.H. Wang, Y.H. Hsieh, L.J. Chen, J. Hazard, Mater. 59 (1998) 251.
[20] R.I. Bickley, T. González-Carreño, L. Palmisano, Mater. Chem. Phys. 29 (1991) 475.
[21] D. Cordrshi, N. Burriesci, F. D'Alba, M. Petrera, G. Polizzoti, M. Schiavello, J. Solid State Chem. 56 (1985) 182.

[22] R.I. Bickley, T. González-Carreño, A.R. González-Elipe, G. Munuera, L. Palmisano, J. Chem. Soc., Faraday Trans. 90 (1994) 2257.
[23] R.I. Bickley, J.S. Lee, R.J.D. Tilley, L. Palmisano, M. Schiavello, J. Chem. Soc., Faraday Trans. 88 (1992) 377.
[24] G. Sankar, K.R. Kannan, C.N.R. Rao, Catal. Lett. 8 (1991) 27.
[25] R.D. Shannon, J. Appl. Phys. 35 (1964) 3414.
[26] A. Nobile Jr., M.W. Davis Jr., J. Catal. 116 (1989) 383.
[27] B.J. Tatarchuk, J.A. Dumesic, J. Catal. 70 (1981) 335.
[28] B.J. Tatarchuk, J.A. Dumesic, J. Catal. 70 (1981) 323.
[29] A. Amorelli, J.C. Evans, C.C. Rowlands, J. Chem. Soc., Faraday Trans. I 85 (1989) 4031.
[30] D. Gazzoli, G. Minelli, M. Valigi, Mater. Chem. Phys. 21 (1989) 93.
[31] J.A. Navío, F.J. Marchena, M. Roncel, M.A. De la Rosa, J. Photochem. Photobiol. A: Chem. 55 (1991) 319.
[32] B. Pal, M. Sharon, G. Nogami, Mater. Chem. Phys. 59 (1999) 254.
[33] P.M. Rao, B. Viswanathan, R.P. Viswanath, J. Mater. Sci. 30 (1995) 4980.
[34] K. Yabe, K. Arata, I. Toyoshima, J. Catal. 57 (1979) 231.
[35] C.R. Brundle, T.J. Chuang, K. Wandelt, Surf. Sci. 68 (1977) 459.